

Supplementary material:
Microrheology of Cells with Magnetic Force Modulation Atomic
Force Microscopy

L. M. Rebêlo, J. S. de Sousa, J. Mendes Filho
Departamento de Física, Universidade Federal do Ceará
Caixa Postal 6030, 60455-760, Fortaleza, Ceará, Brazil,

J. Schäpe, H. Doschke, M. Radmacher
Institut für Biophysik, Universität Bremen
Postfach 330440, D-28334 Bremen, Germany

Contents

1	Magnetic force modulation	2
2	Motion of the free cantilever	4
3	Motion of the cantilever in contact with the sample	5
3.1	Modulation of the contact force and Hertz theory	6
3.2	Comparison of CM1 and CM2 models	7
4	Determination of the sample stiffness	7
5	Phase lag between free and in-contact motions	8
6	Robustness of the model concerning the magnetic cantilever and coil setup	9
7	Comparison with other AFM based micro-rheology methods	10
7.1	Force modulation	10
7.2	Data analysis	10
7.3	Summary of differences between methodologies	12

1 Magnetic force modulation

The basic setup of our AFM force spectroscopy experiment is depicted in Figure 1 of the manuscript. Essentially, we glue a small magnet in the back of a regular AFM cantilever (referred now as *magnetic cantilever*, or MC), and place a coil below the sample stage such that the MC is positioned at a distance x of the coil such that the tip lies in coil axis. Flowing through the coil, there is a AC current of the form:

$$i_{AC}(t) = i_0 \exp i\omega t \quad (1)$$

where ω is the oscillation frequency and i_0 is the current amplitude. The magnetic field in the proximity of the MC can be approximated by the magnetic field of N current loops of radius a at a distance x along their axis, such that:

$$\vec{B}_{AC}(t) = \frac{\mu_0 N i_{AC}(t) a^2}{2(x^2 + a^2)^{3/2}} \hat{x} \quad (2)$$

We can also write $\vec{B}_{AC}(t)$ in terms of the magnetic dipole moment of the coil $\mu_{coil}(t) = (\pi a^2) N i_{AC}(t)$ as:

$$\vec{B}_{AC}(t) = \frac{\mu_0 \mu_{coil}(t)}{2\pi(x^2 + a^2)^{3/2}} \hat{x}, \quad (3)$$

where μ_0 is the vacuum permeability. This AC magnetic field is not uniform since the magnetic field lines outside of the coil are divergent. However, what really matters here is whether the magnet glued to the cantilever will interact with $\vec{B}_{AC}(t)$. Since the MC has a permanent magnetic dipole moment μ_{MC} , the potential energy of μ_{MC} in the presence of $\vec{B}_{AC}(t)$ is given by:

$$U = -\vec{\mu}_{MC} \cdot \vec{B}_{AC}(t) \quad (4)$$

In principle, we do not know which is the direction of $\vec{\mu}_{MC}$, but it will work as long as it has a vertical component to couple with $\vec{B}_{AC}(t)$. Assuming that $\vec{\mu}_{MC} = \mu_{MC} \hat{x}$, an approximate form of force acting on the MC due to $B_{AC}(t)$ is given by:

$$\vec{F}_{AC}(t) = \nabla \left(\vec{\mu}_{MC} \cdot \vec{B}_{AC}(t) \right) \quad (5)$$

Finally, the approximate vertical force acting on the MC located at a distance x above the coil is:

$$\vec{F}_{AC}(t) = -\frac{3}{2\pi} \frac{\mu_0 \mu_{MC} \mu_{coil}(t) x}{(a^2 + x^2)^{5/2}} \hat{x} \quad (6)$$

By expanding the above expression around an average distance x_0 between MC and the coil, we obtain:

$$F_{AC}(x) - F_{AC}(x_0) = -\frac{3\mu_0\mu_{MC}\mu_{coil}(t)}{2\pi} \left[\frac{1}{(a^2 + x_0^2)^{5/2}} - \frac{5x_0^2}{(a^2 + x_0^2)^{7/2}} \right] (x - x_0). \quad (7)$$

Replacing $\mu_{coil}(t) = \pi a^2 i_0 \exp(i\omega t)$, we obtain that the effective driving force on the MC has the form:

$$F_{drive} = G(a, N, i_0, x_0, \mu_{MC})(x - x_0) \exp(i\omega t) = F_B \exp(i\omega t), \quad (8)$$

where the amplitude of the driving force F_B depends on a few parameters of the experimental setup, namely the geometrical characteristics and current amplitude of the coil, and the magnetic dipole moment of the cantilever.

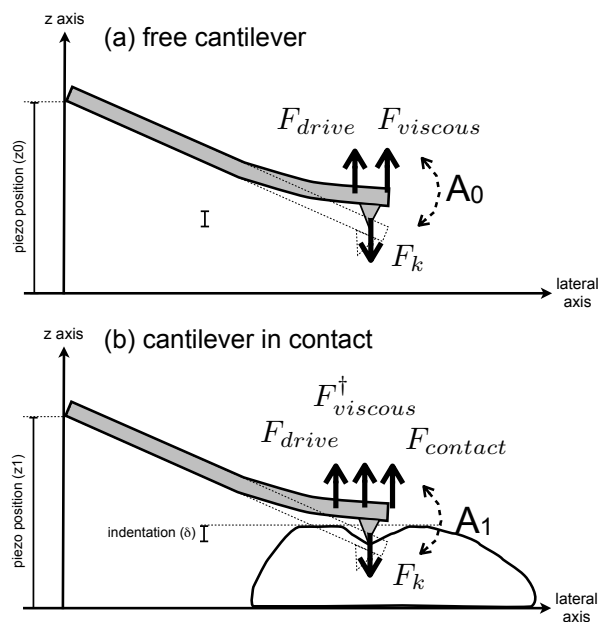


Figure S 1: Schematics of the different forces acting on cantilever immersed in liquid (a) oscillating freely with amplitude A_0 , and oscillating (b) in contact with a viscoelastic sample with amplitude A_1 . F_{drive} indicates the modulating force that makes the cantilever oscillate with a given frequency ω . F_k is the restoring force acting on the deflected cantilever. $F_{viscous}$ describes the viscous interaction of the cantilever with the liquid, $F_{viscous}^\dagger$ is the viscous force due to the liquid + sample, and $F_{contact}$ is the elastic component of contact force between the cantilever and sample.

2 Motion of the free cantilever

Figure S1(a) shows a free MC subjected to an oscillating magnetic field. The resultant force on the MC is given by:

$$F_{total}^{(free)} = F_{drive} + F_k + F_{viscous}, \quad (9)$$

F_{drive} is the oscillating magnetic force, F_k is the restoration force due to the deflected cantilever, which can be described by Hooke's law $F_k = k_c(y - \bar{y})$ (y is the cantilever deflection, and \bar{y} is the equilibrium cantilever deflection), and $F_{viscous}$ represent the viscous forces due to the hydrodynamic interaction of the cantilever with the liquid. The equation of motion for the free cantilever is (assuming $\bar{y} = 0$):

$$m_0 \frac{d^2 y_0(t)}{dt^2} = F_{drive} - k_c y_0(t) - \eta_0 \frac{dy_0(t)}{dt}, \quad (10)$$

where m_0 is the effective mass of the cantilever, k_c is the cantilever spring constant, $y_0(t)$ is the free cantilever deflection, \bar{y}_0 is the free equilibrium deflection. The viscous force was written in the form

$$F_{viscous} = \eta_0 \frac{dy_0(t)}{dt} \quad (11)$$

where η_0 is the hydrodynamic drag coefficient of the free cantilever moving in the liquid. The final differential equation to be solved for the free cantilever is:

$$\frac{d^2 y_0(t)}{dt^2} + b_0 \frac{dy_0(t)}{dt} + \omega_0^2 y_0(t) = F_{drive}/m_0, \quad (12)$$

where $b_0 = \eta_0/m_0$, $\omega_0^2 = k_c/m_0$ is the resonance frequency of the cantilever. This equation represents the well known problem of the driven harmonic oscillator whose solution is of the form:

$$y_0(t) = A_0 \exp(i\omega t + \phi_0) \quad (13)$$

and whose amplitude A_0 and phase angle are respectively given by:

$$A_0 = \frac{F_B}{k_c} \frac{1}{[(1 - (\omega/\omega_0)^2)] + i(b_0\omega/\omega_0^2)}. \quad (14)$$

$$\tan \phi_0 = \text{Im}[A_0]/\text{Re}[A_0]. \quad (15)$$

Figure S2 shows the qualitative dependence of A_0 with ω for different damping regimes. By comparing the experimental behavior of the measured values of A_0 (in Figure 4 of the manuscript) with Fig. S2, we clearly see that measured A_0 fits well in the strongly damped regime where $b_0/\omega_0 > 1$. This explains why we do not observe an increase in A_0 near as ω approaches ω_0 .

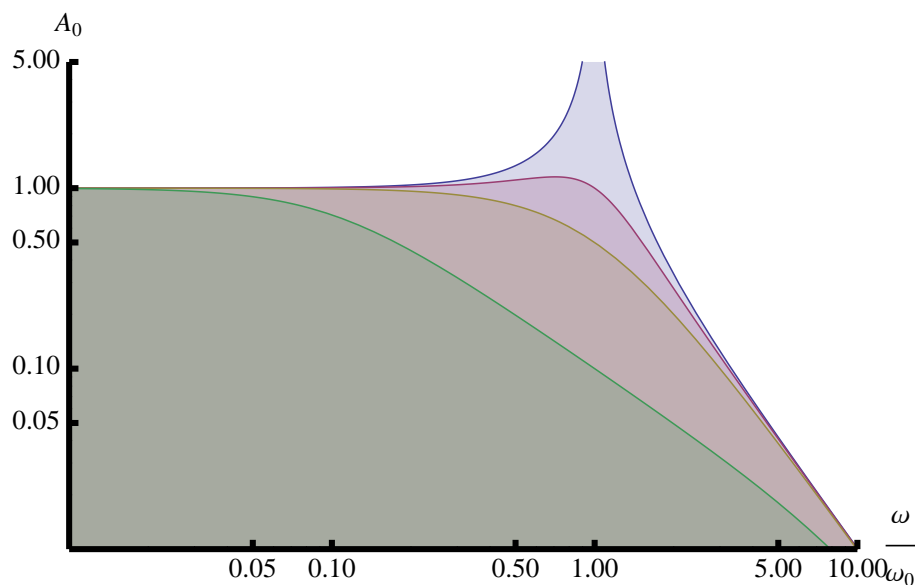


Figure S 2: Dependence of A_0 (in units of F_B/k_c as in Eq. 14) with the driving frequency ω for different damping regimes: from lightest to darkest color, the damping parameter b_0/ω_0 is 0.5, 1.0, 2.0 and 10.0, representing the transition from underdamped to critically damped regimes.

3 Motion of the cantilever in contact with the sample

Figure S1(a) shows a MC in contact with a viscoelastic sample and subjected to an oscillating magnetic field. The resultant force on the MC is given by:

$$F_{total}^{(contact)} = F_{drive} + F_{contact} + F_k + F_{viscous}^\dagger. \quad (16)$$

Therefore, the effective equation of motion of the cantilever in contact $y_1(t)$ is given by:

$$m_1 \frac{d^2 y_1(t)}{dt^2} + \eta_1 \frac{dy_1(t)}{dt} + k_c y_1(t) = F_{drive} + F_{contact}, \quad (17)$$

The viscous force of the contact case is written as

$$F_{viscous}^\dagger = \eta_1 \frac{dy_1(t)}{dt}, \quad (18)$$

where η_1 is the effective hydrodynamic friction coefficient of the liquid + viscoelastic sample.

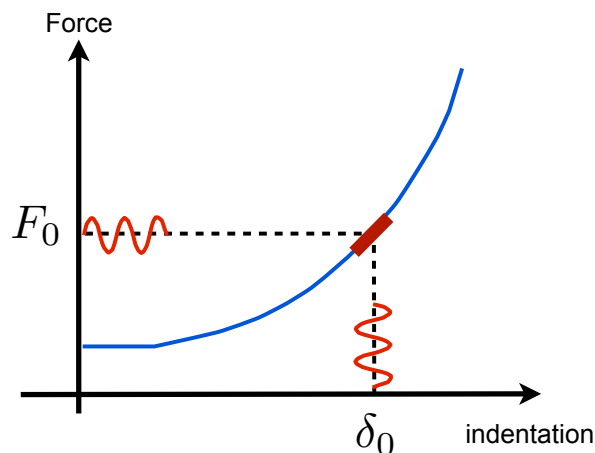


Figure S 3: Schematics of the force modulation of soft samples.

3.1 Modulation of the contact force and Hertz theory

Figure S3 shows the effect of the modulation in the contact force. The experiment is performed such that we first produce an equilibrium indentation δ_0 in the viscoelastic sample, and turn on the sinusoidal modulation with small amplitude which will cause a modulated indentation with the same frequency of the force modulation. The contact force will oscillate around $F_{contact}(\delta_0)$ such that we can expand $F_{contact}(\delta)$ in a Taylor series to determine the effective modulation of the contact force due to the oscillating magnetic field:

$$F_{contact}(\delta) \approx F_{contact}(\delta_0) + F'_{contact}(\delta_0)(\delta - \delta_0) \quad (19)$$

Since the force modulation is directly applied to the cantilever while the piezo stays at rest, we can safely assume that $y_1(t) - \bar{y}_1 = \delta - \delta_0$, where \bar{y}_1 is the initial cantilever deflections that produced the indentation δ_0 . In addition, we note that $k_c \bar{y}_1 = F_{contact}(\delta_0)$. This leads to the alternative form of the equation of motion

$$\frac{d^2 y_1(t)}{dt^2} + b_1 \frac{dy_1(t)}{dt} + \omega_1^2 (y_1(t) - \bar{y}_1) = F_{drive}/m_0, \quad (20)$$

where $b_1 = \eta_1/m_0$ and $\omega_1^2 = [\omega_0^2 + F'_{contact}(\delta_0)/m_0] = \omega_0^2 [1 + F'_{contact}(\delta_0)/k_c]$. This equation states that the contact of the cantilever with the viscoelastic surface induces a small change in the resonance frequency. To estimate $F'_{contact}(\delta_0)$, we make use of the Hertz theory for pyramidal indenters:

$$F_{contact} = \frac{1}{\sqrt{2}} E' \delta^2 \tan \theta, \quad (21)$$

where $E' = E/(1 - \nu^2)$. ν represents the Poisson ratio of the sample, and θ is the half-opening angle of the cantilever tip. Then, we obtain $F'_{contact}(\delta_0) = \sqrt{2}E' \tan \theta \delta_0$. Since, the E and ν are two unknown quantities, we can estimate $F'_{contact}(\delta_0) = 2F_{contact}(\delta_0)/\delta_0 = k_c d_{trigger}/\delta_0$. δ_0 is easily determined by measuring a traditional force curve just before the frequency-modulated measurement. For $k_c = 0.01$ N/m and $d_{trigger} = 0.2$ μm , typical values of indentations δ_0 range between 1.0 - 2.0 μm , depending on the cell. Therefore, the values of $F'_{contact}(\delta_0)/k_c$ range between 0.1 - 0.2. Finally, The solution of Eq. 20 is:

$$y_1(t) = \bar{y}_1 + A_1 \exp(i\omega t + \phi_1), \quad (22)$$

3.2 Comparison of CM1 and CM2 models

Note that we have two equivalent model equations given by Eqs. 17 and 20. The former exhibits explicitly the effective contact force given by Eq. 19, and the latter just assumes that the effect of contact modifies the resonance frequency of the cantilever. Those models are labeled as CM2 and CM1, respectively in the manuscript. The idea behind CM2 is to describe the effective motion of the cantilever with minimum number of parameters, while the idea behind CM1 is to compared the measured solution with actual force contact details used in the experiment. and whose amplitude A_1 is given by :

$$A_1^{(CM1)} = \frac{F_B}{k_c} \frac{1}{[1 + (F'_{contact}(\delta_0)/k_c) - (\omega/\omega_1)^2] + i(b_1\omega/\omega_0^2)}, \quad (23)$$

$$A_1^{(CM2)} = \frac{F_B}{k_c + k_s} \frac{1}{[(1 - (\omega/\omega_1)^2) + i(b_1\omega/\omega_1^2)]}, \quad (24)$$

4 Determination of the sample stiffness

In the previous sections, we described the motion of the cantilever free and in contact with a viscoelastic sample in terms of the solution of the driven harmonic oscillator. The most striking differences between the cantilever motions are: (i) the oscillation amplitudes are different, being A_0 for the free cantilever and A_1 for the cantilever in contact with a viscoelastic sample. (ii) The resonance frequencies and phase angles for both motions are also different ($\omega_0 \neq \omega_1$ and $\phi_0 \neq \phi_1$).

To estimate the sample stiffness we simplify both free and in-contact motion by a simple arrangement of springs. This is shown in Fig. 4. The free motion is described by a mass connected to a single spring (representing the cantilever). The in-contact motion can be described by a mass connected to two springs (representing the cantilever and sample). Assuming that we pull down the mass with a given force F_B in both systems (e.g., the magnetic force). In the free cantilever model, the displacement is A_0 . For the in-contact system, since the same force has to deform two springs, we obtain a smaller displacement A_1 ($A_1 < A_0$). By equating the forces, we obtain

$k_c A_0 = (k_c + k_s) A_1$, which leads to a sample stiffness k_s that can be determined in terms of A_0 and A_1 with:

$$k_s = k_c \left(\frac{A_0}{A_1} - 1 \right). \quad (25)$$

For a very stiff sample, no indentation will occur, thus the amplitude in contact A_1 will be zero, leading to $k_s \rightarrow \infty$. For a very soft sample, the amplitude in contact $A_1 \rightarrow A_0$, which leads to $k_s \rightarrow 0$.

In the limit of $\omega \rightarrow 0$ we have only elastic response because the viscous components $dy_n/dt \rightarrow 0$. By replacing this limit in Eqs. 14 and 23, we obtain Eq. 10 of the manuscript. For $\omega > 0$, viscous effects are present, and k_s represents an effective spring constant.

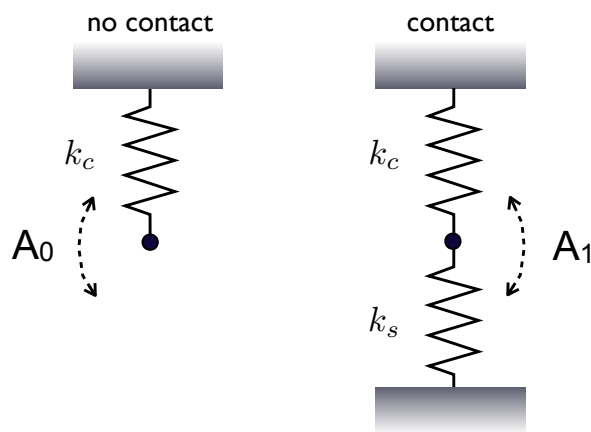


Figure S 4: Association of springs to determine the effective sample stiffness k_s in terms of the cantilever stiffness k_c , and the oscillation amplitudes A_0 and A_1 .

5 Phase lag between free and in-contact motions

The phase lag ϕ between the cantilever motions, which are directly related to the internal viscosity of the sample, is calculated by

$$\phi = \phi_1 - \phi_0. \quad (26)$$

The phase angles of each type of cantilever motion is

$$\tan \phi_n = \text{Im}[A_n]/\text{Re}[A_n] \quad (27)$$

For small angles, one has within the CM2 approach:

$$\tan \phi_n \approx \phi_n = b_n \omega / (\omega^2 - \omega_n^2). \quad (28)$$

We can make a further approximation assuming $\omega_1 \approx \omega_0$ to determine the phase difference as:

$$\phi \approx \frac{(b_1 - b_0)\omega}{\omega^2 - \omega_0^2} \quad (29)$$

Since b_1 describes the viscous damping due to liquid + sample, and b_0 is only due to the liquid, the phase difference ϕ carries only the information about the viscosity of the sample.

6 Robustness of the model concerning the magnetic cantilever and coil setup

The amplitudes $A_0(\omega)$ and $A_1(\omega)$ are the main quantities to extract the effective sample stiffness. Besides the well known frequency dependency, they also contain a dependence on the amplitude of the magnetic force F_B , which was described in Section 1.

Since the sample stiffness k_s is a function of the ratio A_0/A_1 , the F_B term in the numerator of both A_0 and A_1 are cancelled. This effectively eliminates the dependence of the model on the magnetic dipole moment of the cantilever μ_{MC} . *The main important ingredient here is that the magnetic force is strong enough to produce a deflection in the cantilever.*

Another important parameter of the experimental design is the current amplitude i_0 flowing through the coil. Since the coil circuit is an oscillator itself, it also has its own resonance frequency ω_{coil} and frequency-dependent amplitude $i_0(\omega)$ similar to $A_{0,1}(\omega)$. Therefore, the coil circuit has dramatical influence in the ability to obtain good cantilever deflections.

One should also note that the current amplitude $i_0(\omega)$ is the same for both free and in-contact motions of the cantilever. In the individual measurements of $A_0(\omega)$ and $A_1(\omega)$, we have to be aware that two resonance frequencies may play a role: the cantilever resonance frequency ω_n and the coil resonance frequency ω_{coil} . However, the influence of the coil resonance is cancelled in the ratio $A_0(\omega)/A_1(\omega)$, removing away its influence in the determination of both samples stiffness k_s and phase angles ϕ_n , which are the aimed quantities of our theory.

The critical details of our experimental setup are:

- The aimed range of frequencies that samples will be subjected must avoid the resonance frequencies ω_0 and ω_{coil} because the amplitude A_0 can decrease to very small values. The former can be determined by the well known thermal method, and the latter can be monitored by measuring $A_0(\omega)$.
- $A_0(\omega)$ must exhibit a curve similar to Fig. S2. If some resonance frequency appear in the measurement, one simple method to rule out wheter this resonance is due to the coil is to measure $A_0(\omega)$ in and out of the liquid. The added mass of the liquid does not influence ω_{coil} .

- The most important requirement is to produce a sufficient amplitude oscillation of the MC to indent the viscoelastic sample. By sufficient, we mean that both A_0 and A_1 must be unequivocally larger than average thermal oscillation amplitude A_{th} , which can be estimated as $\langle A_{th} \rangle = \sqrt{k_B T / k_c}$. For room temperature and $k_c = 0.01$ N/m, we obtain: $\langle A_{th} \rangle \approx 1.0$ nm. By imposing a comfortable confidence margin, let's assume that $A_1 \geq 5\langle A_{th} \rangle$. For soft samples whose stiffnesses range from $0.1k_c$ to $1.0k_c$, Eq. 25 indicates that a value of $A_0 \approx 10$ nm is more than enough.

7 Comparison with other AFM based micro-rheology methods

There is another AFM based approach to perform micro-rheology experiments in soft samples (1, 2). The main differences between this and our methodology are: (i) force modulation method, and (ii) physical model used in the data analysis. These differences will be described individually in this section.

7.1 Force modulation

The main difference between this and our experimental setup is depicted in the Fig. S5. In our setup, the force modulation is applied directly to the MC, which is in contact with the sample. This guarantees that the only phase lag between the magnetic force modulation F_{drive} and the corresponding cantilever oscillation is due to the viscosity of the liquid and sample. As for the common setup found the literature, the force modulation is achieved by modulating the piezo actuator that controls the distance between the sample and the cantilever tip. In this case, it is necessary first to remove the phase lag of the piezo actuator, which could induce an error in the determination of the viscoelastic properties of the sample, as pointed out by Alcaraz et al. (3). Another striking difference between both experimental setups is that we construct our $k_s(\omega)$ curves by applying a single frequency per time, while the other approach generates a piezo modulation with several frequencies spanning in several frequency decades. The frequency-dependent shear moduli curves $G(\omega)$ are obtained by performing a Fourier analysis of the measured quantities.

7.2 Data analysis

The force modulation in Fig. S5(b) is obtained by modulating the distance between the sample and cantilever with $z(t) = \bar{z} \exp i\omega t$. The corresponding cantilever deflection is given by $y(t) = y_0 + \bar{y} \exp(i\omega t + \phi)$, where ϕ is the phase lag due to the internal viscosity of the sample. The sample indentation is obtained by $\delta(t) = z(t) - y(t)$, which is also an oscillating quantity of the form $\delta(t) = \delta_0 + \bar{\delta} \exp(i\omega t + \phi)$. The model equation to describe the cantilever motion is:

$$m_0 \frac{d^2 y(t)}{dt^2} + k_c y(t) = F_{contact} + F_{visco}. \quad (30)$$

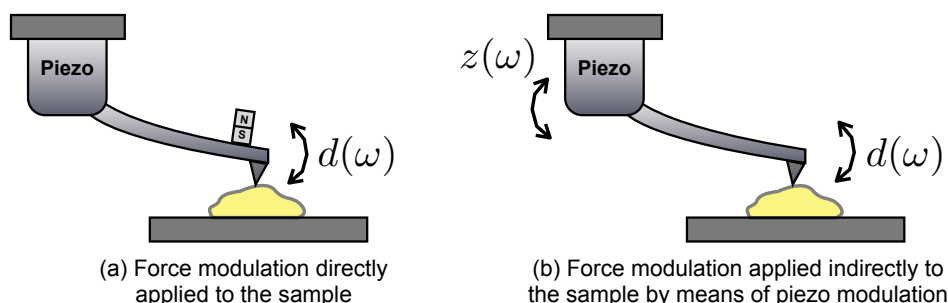


Figure S 5: Comparison of AFM-based force modulation methods. In (a) the force modulation is directly applied to the MC by means of an external oscillating magnetic field. In (b) the force modulation is obtained by modulating the piezo actuator that controls the distance between the sample and the cantilever.

In the frequency domain, this equation reads:

$$\left(1 - \frac{\omega^2}{\omega_0^2}\right) k_c y(\omega) = F_{contact}(\omega) + F_{visco}(\omega). \quad (31)$$

By using the hydrodynamic drag model of Alcaraz *et al.* (3), one has:

$$F_{visco}(\omega) = b(0) d\delta/dt = ib(0)\omega\delta(\omega) \quad (32)$$

Assuming that the aimed range of frequencies to which the samples will be subjected is much smaller than the resonance frequency ω_0 , one obtains:

$$k_c y(\omega) \approx F_{contact}(\omega) + ib(0)\omega\delta(\omega). \quad (33)$$

By expanding the Hertz model (Eq. 21) around the equilibrium indentation δ_0 we obtain an expression similar to Eq. 19.

$$F_{contact}(\delta) = F_{contact}(\delta_0) + \frac{\sqrt{2} \tan \theta \delta_0 E}{(1 - \nu)^2} (\delta - \delta_0). \quad (34)$$

By noticing that the shear modulus is related to the Young modulus as $G = E/2(1 + \nu)$, the Fourier transform of $F_{contact}$ becomes:

$$F_{contact}(\omega) = \frac{2\sqrt{2}\delta_0 \tan \theta}{(1 - \nu)} G(\omega) \delta(\omega). \quad (35)$$

The frequency-dependent shear modulus is obtained with:

$$G(\omega) = \frac{(1 - \nu)k_c}{2\sqrt{2}\delta_0 \tan \theta} \left[\frac{y(\omega)}{\delta(\omega)} - i \frac{b(0)\omega}{k_c} \right]. \quad (36)$$

Equation 36 is the main expression used in references (1, 2) to obtain the shear modulus of the viscoelastic samples. Essentially, they measure the time-dependent motion of the piezo actuator $z(t)$ and signal of the cantilever deflection $y(t)$ to construct the dynamical indentation $\delta(t) = z(t) - y(t)$. By plugging the hydrodynamic drag coefficient $b(0)$ (see Ref. (3)) and the FFT of $y(t)$ and $z(t)$ in Eq. 36, one obtains the frequency-dependent complex shear modulus of the viscoelastic samples. The storage $G'(\omega)$ and loss $G''(\omega)$ moduli are easily obtained with $G'(\omega) = \text{Re}[G(\omega)]$ and $G''(\omega) = \text{Im}[G(\omega)]$, respectively. The phase lag is obtained with $\tan \phi(\omega) = G''(\omega)/G'(\omega)$.

The most notable difference between our model and the one described above is that our methodology aims to determine the frequency-dependent sample stiffness $k_s(\omega)$ and the phase angle $\phi(\omega)$, while the method above aims to determine the complex shear modulus $G(\omega)$.

It is possible to demonstrate that both models are equivalent. From Eq. 19, one can easily obtain that the sample stiffness at the indentation δ_0 is given by:

$$k_s = \frac{F_{\text{contact}}(\delta) - F_{\text{contact}}(\delta_0)}{\delta - \delta_0} = F'_{\text{contact}}(\delta_0). \quad (37)$$

By plugging Hertz model for conical indenters above, one obtains:

$$k_s = \frac{2\sqrt{2} \tan \theta \delta_0}{1 - \nu} G, \quad (38)$$

where $G = E/[2(1 + \nu)]$. The above expression shows that the stiffness k_s and the shear modulus G are related to each other by a length factor (δ_0), by the indenter geometry, and by the Poisson ratio of the sample. With the help of Eq. 25, G can be written in terms of A_0 and A_1 :

$$G = \frac{1 - \nu}{2\sqrt{2} \tan \theta \delta_0} \left[k_c \left(\frac{A_0}{A_1} - 1 \right) \right]. \quad (39)$$

7.3 Summary of differences between methodologies

The main differences between both methodologies are summarised below:

- Our method applies the force modulation directly to the indenter, while the other methodology modulates the distance $z(t)$ between the sample and cantilever in order to generate a modulated indentation $\delta(t)$. This requires the removal of the phase lag due to the piezo and electronic circuitry of the AFM.
- The hydrodynamic drag due to the liquid is naturally included in our methodology, while in the other approach one must know *a priori* the hydrodynamic drag factor $b(0)$ in order to

determine the complex shear modulus in Eq. 36. The method to obtain $b(0)$ is described in detail by Alcaraz et al. (3).

- Our methodology aims to obtain the phase lag ϕ and stiffness k_s which is related to the shear modulus G by Eq. 38, while the other methodology directly determine the storage G' and loss G'' shear moduli.
- Since k_s and G are connected to each other by a simple length factor and by the indenter geometry, both must exhibit the same frequency-dependent behavior. However, determining k_s involves no previous knowledge of the indenter geometry, Poisson ratio nor the hydrodynamic factor $b(0)$.

References

- [1] Alcaraz, J., L. Buscemi, M. Grabulosa, X. Trepas, B. Fabry, R. Farré, and D. Navajas, 2003. Microrheology of human lung epithelial cells measured by atomic force microscopy. *Biophys. J.* 84:2071.
- [2] Mahaffy, R. E., S. Park, E. Gerde, J. Käs, and C. K. Shih, 2004. Quantitative Analysis of the Viscoelastic Properties of Thin Regions of Fibroblasts Using Atomic Force Microscopy. *Biophys. J.* 86:1777.
- [3] Alcaraz, J., L. Buscemi, M. P. de Morales, J. Colchero, A. Baró, and D. Navajas, 2002. Correction of microrheological measurements of soft samples with atomic force microscopy for the hydrodynamic drag on the cantilever. *Langmuir* 18:716.